Journal of Cranio-Maxillo-Facial Surgery 47 (2019) 468–472

Contents lists available at ScienceDirect

Journal of Cranio-Maxillo-Facial Surgery

journal homepage: www.jcmfs.com

Analysis of simulated mandibular reconstruction using a segmental mirroring technique

Joel C. Davies [1], Harley H.L. Chan [1], Yelda Jozaghi, David P. Goldstein, Jonathan C. Irish*

Department of Otolaryngology, Head & Neck Surgery/Surgical Oncology, Princess Margaret Cancer Centre and Guided Therapeutics (GTx) Program, University of Toronto, Toronto, Ontario, Canada

ARTICLE INFO

Article history:
Paper received 12 November 2018
Accepted 21 December 2018
Available online 30 December 2018

Keywords:
3D modeling
Mandibular reconstruction
Computer simulation

ABSTRACT

Purpose: When deforming pathology limits intraoperative plating of the mandible, three-dimensional (3D) models can be generated by digitally replacing the deformed segment of bone with an inverted segment from the contralateral unaffected mandible to adapt a reconstruction plate. The purpose of this study was to use 3D conformance analysis to evaluate the degree of accuracy of this "segmental mirroring" technique.

Methods: Using a pre-existing melanoma database (January 1, 2005–September 20, 2015), high-resolution computed tomography (CT) scans of the head and neck were obtained from patients without evidence of bony disease or defects involving the mandible. Using 3D software (Mimics, Materialise, Leuven, Belgium), each mandible was segmented based on four defect classes (Ic, II, IIc and III) of the Brown et al. (2016) classification system. An inverted, or "mirrored", image of each segment was digitally created and manually co-registered with the corresponding contralateral segment of the mandible. Conformance analysis was performed by calculating the root-mean-square (RMS) conformance distance and through evaluating 3D generated conformance maps. The primary outcome was degree of conformance. Data were analyzed using descriptive statistics and tests of statistical significance. The significance level was set at a p-value less than or equal to .05.

Results: A high degree of conformance (mean RMS < 1 mm) was observed when comparing all classes of simulated reconstruction. The closest conformance was observed for class III simulated reconstructions (mean RMS: 0.4 ± 0.2 mm). Inclusion of the condyle resulted in a reduced mean RMS conformance (class II: 0.5 ± 0.3 mm vs class IIc: 0.7 ± 0.5 mm; $p = 0.01$). There was no significant difference between RMS conformance distances when comparing side of simulated reconstruction. Evaluation of 3D mapping demonstrated reduced conformance with simulated reconstruction of the condyle and coronoid process.

Conclusion: The segmental mirroring technique can be used reliably to generate highly accurate three-dimensional models that may assist with mandibular reconstruction in circumstances where bony deformity limits intraoperative adaptation of a reconstruction plate. This technique is less accurate where pathology involves the mandibular condyle and, to a lesser degree, the coronoid process.

Crown Copyright © 2019 Published by Elsevier Ltd on behalf of European Association for Cranio-Maxillo-Facial Surgery. All rights reserved.

1. Introduction

A primary goal of oromandibular reconstruction is to preserve function through re-establishing mandibular continuity and maintaining symmetric contour (Cohen et al., 2009). Deforming pathologic processes of the mandible pose unique challenges to reconstructive surgeons as achieving optimal contour is necessary for restoring normal occlusion, which is influenced by the degree of deformation. Intraoperative adaptation of a reconstruction plate over a distorted segment of bone will result in an inadequate fit between the plate and bone graft potentially leading to malocclusion, temporomandibular joint dysfunction and an increased risk for plate extrusions (Abou-elfetouh et al., 2011; Li et al., 2011; Lee et al., 2007). However, this is also dependent on the extent and location of defect following resection (Brown et al., 2016).

* Corresponding author.
E-mail addresses: joel.davies@mail.utoronto.ca (J.C. Davies), jonathan.irish@uhn.ca (J.C. Irish).

[1] The first two authors (Joel C Davies and Harley HL Chan) equally contributed to the production of this manuscript.

https://doi.org/10.1016/j.jcms.2018.12.016
1010-5182/Crown Copyright © 2019 Published by Elsevier Ltd on behalf of European Association for Cranio-Maxillo-Facial Surgery. All rights reserved.

A recently developed technique involves digitally removing a tumor of the mandible using a CT generated three-dimensional (3D) computer model, filling the defect with a "mirrored", or inverted, image of the unaffected contralateral segment of the mandible and printing a 3D stereolithographic model to bend a reconstruction plate. While this technique has been reported in various case studies to be successful in reconstruction of the mandible secondary to deforming tumors (e.g. ameloblastoma, etc), trauma and osteoradionecrosis, no study has examined the accuracy of this method using quantitative parameters based on the classification of defect (Cohen et al., 2009; Lee et al., 2007; Hannen, 2006; Khalifa et al., 2016; Singare et al., 2004).

Numerous systems have been proposed for classifying mandibular defects resulting from segmental mandibulectomy. More recently, Brown et al. (2016) developed a classification system based on the most commonly encountered defects following oncologic resection (Brown et al., 2016). This system categorizes defects into four classes with subclasses for inclusion of the mandibular condyle (Table 1). The location and extent of resection often dictates the type of osteocutaneous/osseous free flap reconstruction. Other factors in determining type of flap include age, comorbidities, occupational/recreational activities and decisions regarding dental rehabilitation. The fibular, scapular and iliac crest free flaps are among the most commonly selected (Brown et al., 2016).

The objective of the study was to determine the degree of conformance between simulated mandibular defects, based on the Brown et al. (2016) classification system, and the corresponding inverted segments of the contralateral mandible using high resolution CT generated 3D computer models.

2. Materials & methods

2.1. Study design and sample selection

The study population was comprised of patients randomly selected from an institutional melanoma database between January 1, 2005 and September 30, 2015 (Princess Margaret Cancer Centre, Department of Otolaryngology, University Health Network). To be included in the study, patients must have completed high resolution CT imaging of the head/neck with minimal metal artifacts from dentures and fillings. Patients were excluded from the study if there was evidence of bony disease involving the mandible and severe image artifacts. Institutional research ethics board approval was obtained for this study.

2.2. Study variables

For each patient, conformance between a segment of the mandible, and the corresponding contralateral segment, was measured quantitatively as the mean root-mean-square (RMS) conformance distance (mm) and through analyzing 3D conformance mapping with associated variations in conformance distances. As described in our prior studies, the RMS conformance distance provides a metric for morphologic similarity (Lee et al., 2007; Brown et al., 2016). Other demographic variables included age and sex.

2.3. Data collection

High resolution CT scans were acquired using multi-detector CT (Aquilion 64, Toshiba) with standard protocols exhibiting nearly isotropic 3D spatial resolution for the facial bones. The image voxel size was 0.47 mm^3. The protocols for head and neck CT imaging at our institution include: helical scan mode, a peak voltage of 120 kVp and an X-ray current set at automatic exposure control (maximum: 450 mA; minimum: 50 mA).

Using a method devised in our laboratory, conformance analysis was performed as described previously (Pagedar et al., 2012; Chan et al., 2010). The images were imported to a workstation and semi-automatic segmentation was performed using Mimics version 18.0 (Materialise, Leuven, Belgium) 3D visualization software. Bone and soft tissue were differentiated by intensity threshold. Regions of bone specific to the mandible were segmented. Following manual editing and smoothing, the segmentations were converted to mesh models and imported to 3-matic version 11.0 (Materialise, Leuven, Belgium).

The areas of bone encompassing defect classes Ic, II, IIc and III were virtually isolated via segmentation, inverted using 3D software (3-matic version 11.0 – Materialise, Leuven, Belgium) and merged with the corresponding areas of the contralateral mandible (Fig. 1). The plane of inversion was the sagittal (YZ) plane and mirrored models were manually initiated by overlapping the models followed by automatic co-registration with the contralateral segments. Conformance analysis was completed to determine the degree of morphologic similarity between the inverted image and the contralateral mandible for each defect class.

Using calculated radiographic volumes, conformance maps were generated as previously described (Pagedar et al., 2012; Chan et al., 2010). The volumes of each bone segment were transformed into triangular lattices, and conformance distances between the surfaces of the segmented objects were calculated. These were determined by calculating the distance between each vertex point on the inverted mandibular segment and the nearest three vertices on the corresponding contralateral mandible. Color-coded maps illustrating the range of these distances were created to delineate the extent of conformance (Fig. 2). We analyzed eight different reconstructive scenarios for each patient: bilateral classes Ic, II, IIc and III. Given that preliminary data demonstrated no difference between classes I and II, only class II was included. We did not include class IV and V simulated reconstructions due to the extent of the defect involving a substantial amount of bone on either side of the midline of the mandible, resulting in an inability to generate a 3D model.

2.4. Data analysis

Mean conformance distances were compared between the four defect classes. The root-mean-square (RMS) conformance, a metric for morphologic similarity (Pagedar et al., 2012; Chan et al., 2010), was calculated for each comparison. Paired t-tests were performed

Table 1
Classification of mandibular defects (adapted from Brown et al., 2016).

Class	Description
I (angle)	Lateral defect not including ipsilateral canine or condyle
Ic (angle & condyle)	Lateral defect including condyle
II (angle & canine)	Hemi-mandibulectomy including ipsilateral, but not contralateral canine or condyle
IIc (angle, canine & condyle)	Hemi-mandibulectomy including condyle
III (both canines)	Anterior mandibulectomy includes both canines, but neither angle
IV (both canines & at least one angle)	Extensive anterior mandibulectomy including both canines and one or both angles
IVc (both canines & at least one condyle)	Extensive anterior mandibulectomy including both canines and one or both condyles

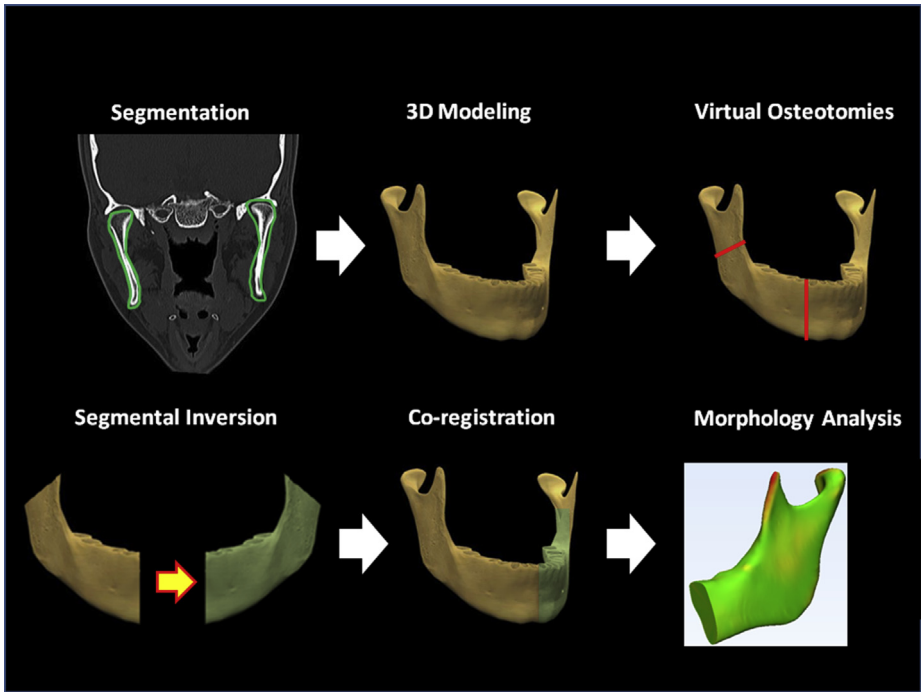

Fig. 1. Sequence utilized to generate and analyze three-dimensional mandibular models using inverted bony segments.

to test for a difference between the various reconstructive scenarios. P-values less than 0.05 were deemed statistically significant. All descriptive statistics were calculated with SAS 9.3 (SAS Institute, Cary, NC, USA).

3. Results

This retrospective cross-sectional study included a total of 10 patients (6 males, 4 females; mean age 55 ± 18; age range 31–85) that met criteria for inclusion and exclusion.

3.1. Class of reconstruction

Overall, a high degree of conformance (<1 mm difference between sites of reconstruction) was observed when comparing all classes of simulated reconstruction (Table 2 and Fig. 2). A mean RMS conformance measurement greater than 1 mm was only observed in one patient (P9) for simulated reconstruction of the right hemimandible using mandibular segments that included the condyle (class Ic: 1.1 ± 0.7 mm; class IIc: 1.1 ± 0.7 mm). Conformance varied dependent on the class of reconstruction with the highest conformance for class III simulated reconstructions (Mean RMS: 0.4 ± 0.2 mm; Range: 1×10^{-4}–2.6 mm) and lowest conformance for class IIc reconstructions (Mean RMS: 0.7 ± 0.5 mm; Range: 1×10^{-4} – 3.1 mm). Class III reconstruction had significantly improved conformance compared to classes Ic ($p < 0.01$), II ($p < 0.01$) and IIc ($p < 0.01$). Inclusion of the condyle within the simulated reconstruction resulted in a significantly reduced mean RMS conformance (class II: 0.5 ± 0.3 mm vs class IIc: 0.7 ± 0.5 mm; $p = 0.01$). There was no significant difference between RMS conformance distances when comparing side of simulated reconstruction for any of the classes examined (Ic: $p = 0.74$; II: $p = 0.90$; IIc: $p = 0.66$; III: $p = 0.59$).

3.2. Conformance mapping

Conformance mapping of the simulated reconstructions demonstrated excellent conformance along the ramus, body and symphysis of the mandible (Fig. 3). The overall mean minimum conformance measurement across these areas was 1×10^{-3}mm. Conversely, areas of reduced conformance included the condyle and superior aspect of the coronoid process with an overall mean maximum conformance of 2.87 mm.

4. Discussion

Given that segmental mirroring has been reported as a successful technique within case reports in the literature, our hypothesis was that a high degree of conformance would be observed, but that variability would exist dependent on defect class of the mandible to be simulated for reconstruction (Cohen et al., 2009; Lee et al., 2007; Hannen, 2006; Khalifa et al., 2016; Singare et al., 2004). This was borne out by the data which demonstrated that mirrored segments from each of the four classes analyzed achieved a level of conformance within 1 mm. Despite a high level of conformance, variations were found to exist. Models that included the condyle demonstrated reduced conformance. Although a 3D generated model of the condyle itself would not be used to adapt a reconstruction plate, it is possible that the positioning of the condyle within the glenoid fossa may be altered due to the observed asymmetry between sides. This must be taken into consideration when pre-planning for surgery including condylar defects. Although we found that modeling of class III reconstructions using the mirroring technique had the highest degree of conformity, it is important to note that this relates to the model itself. Therefore, while a plate bent to a model of this area may be very accurately contoured, multiple osteotomies of a selected bone graft may be required to fit this contour. The reconstruction plate can serve as a guide for planning osteotomies, but it is the match of the bone graft, and not the reconstruction plate, that determines the success of reconstruction.

Conformance mapping in prior studies has been useful in analyzing locations of maximal and minimal conformance between co-registered sites of three-dimensional models (Pagedar et al., 2012; Chan et al., 2010). Our study demonstrated that the mandibular ramus, body and symphysis had maximal

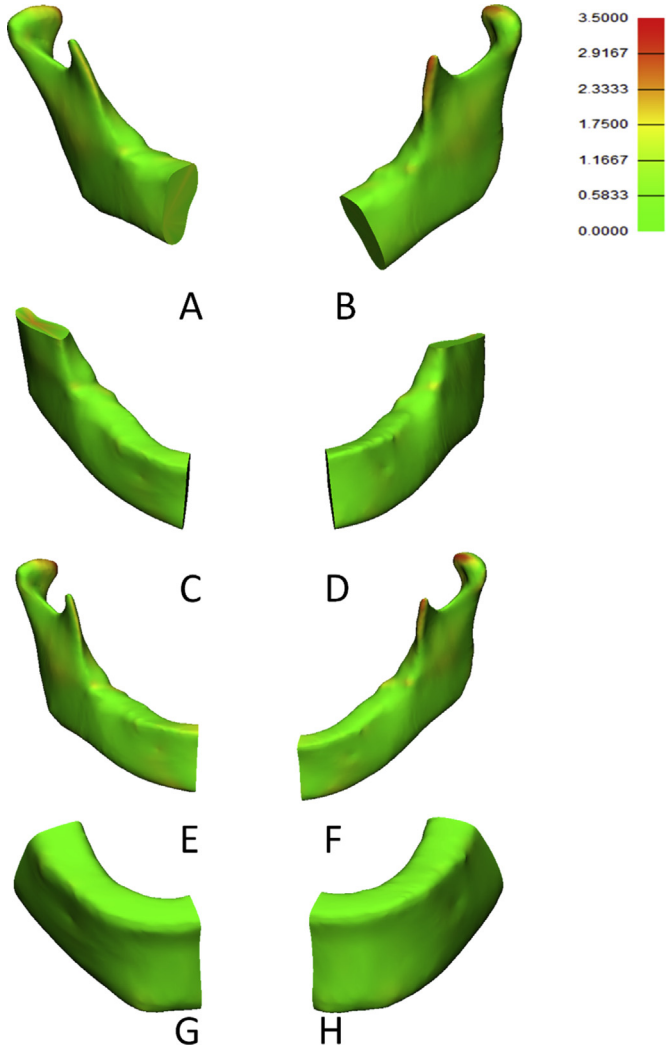

Fig. 2. An example of three-dimensional reconstructions of the mandible from one patient (P4) demonstrating conformance mapping between corresponding segments of bone including class Ic **(A & B)**, class II **(C & D)**, class Ic **(E & F)** and class III **(G & H)**. Color-coding indicates areas of maximal conformance in green, moderate conformance in yellow, and poor conformance in red (RMS conformance distance – mm).

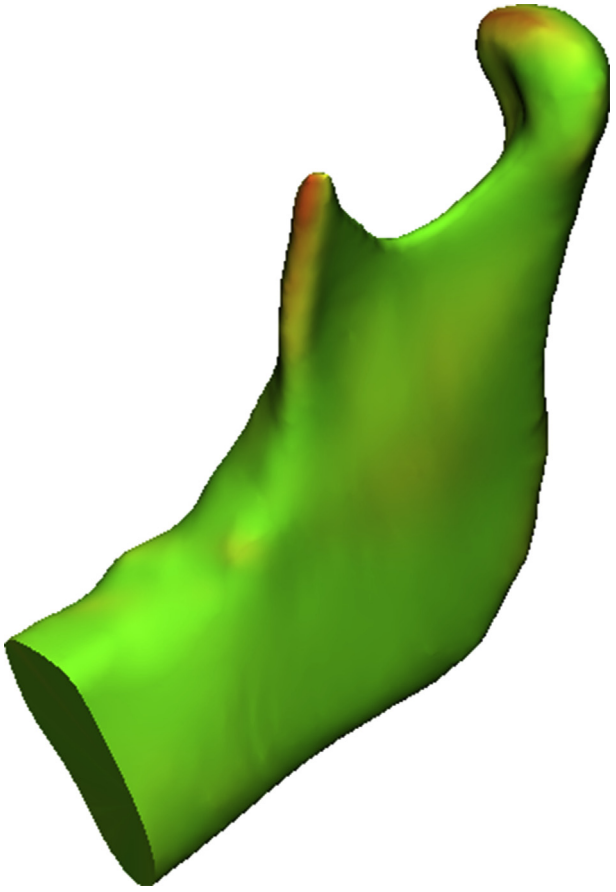

Fig. 3. An example of a simulated class Ic three-dimensional reconstruction of the left hemimandible using a corresponding segment from the contralateral right hemimandible in one patient (P4). Optimal contour is demonstrated along the mandibular ramus and body, with reduced conformance involving the coronoid process and condyle. Color-coding indicates areas of maximal conformance in green, moderate conformance in yellow, and poor conformance in red.

conformance. These areas are geometrically less complex with long linear segments of bone and therefore are more easily modeled and reconstructed. Conversely, the mandibular condyle, and to a lesser extent, the coronoid process, are more complex anatomic regions and demonstrate reduced conformance. The mandibular condyle has been acknowledged in the literature as a challenging area of reconstruction and has important implications for functional

Table 2
Root-mean-square conformance distances (mm) for simulated reconstructions of four mandibular defect classes[a] using contralateral inverted mandibular segments (n = 10).

Patient	RMS Conformance distance (mm)							
	Reconstructed left mandibular defect with inverted right mandibular segment				Reconstructed right mandibular defect with inverted left mandibular segment			
	Ic	II	IIc	III	Ic	II	IIc	III
1	0.6 ± 0.4	0.6 ± 0.4	0.6 ± 0.4	0.4 ± 0.2	0.6 ± 0.4	0.5 ± 0.3	0.6 ± 0.4	0.4 ± 0.2
2	0.8 ± 0.6	0.8 ± 0.6	0.8 ± 0.6	0.5 ± 0.4	0.9 ± 0.6	0.8 ± 0.5	0.8 ± 0.6	0.4 ± 0.3
3	0.6 ± 0.4	0.5 ± 0.3	0.7 ± 0.4	0.3 ± 0.2	0.6 ± 0.4	0.5 ± 0.3	0.7 ± 0.4	0.3 ± 0.2
4	0.6 ± 0.4	0.5 ± 0.3	0.6 ± 0.4	0.4 ± 0.2	0.7 ± 0.5	0.5 ± 0.3	0.7 ± 0.4	0.3 ± 0.2
5	0.8 ± 0.5	0.7 ± 0.4	0.8 ± 0.5	0.4 ± 0.2	0.8 ± 0.5	0.7 ± 0.5	0.9 ± 0.6	0.4 ± 0.2
6	0.6 ± 0.4	0.6 ± 0.4	0.7 ± 0.4	0.4 ± 0.2	0.6 ± 0.3	0.6 ± 0.4	0.6 ± 0.4	0.3 ± 0.2
7	0.7 ± 0.5	0.5 ± 0.3	0.7 ± 0.5	0.3 ± 0.2	0.7 ± 0.4	0.5 ± 0.3	0.7 ± 0.5	0.3 ± 0.2
8	0.6 ± 0.4	0.5 ± 0.3	0.6 ± 0.4	0.5 ± 0.3	0.6 ± 0.4	0.6 ± 0.4	0.6 ± 0.4	0.4 ± 0.3
9	0.9 ± 0.6	0.7 ± 0.4	1.0 ± 0.6	0.4 ± 0.3	1.1 ± 0.7	0.6 ± 0.4	1.1 ± 0.7	0.4 ± 0.3
10	0.6 ± 0.4	0.4 ± 0.2	0.6 ± 0.4	0.4 ± 0.3	0.5 ± 0.3	0.4 ± 0.2	0.5 ± 0.4	0.4 ± 0.2
TOTAL	**0.7 ± 0.4**	**0.6 ± 0.4**	**0.7 ± 0.5**	**0.4 ± 0.3**	**0.7 ± 0.5**	**0.6 ± 0.4**	**0.7 ± 0.5**	**0.4 ± 0.2**

[a] Brown et al. (2016) classification of mandibular defects.

outcomes (Brown et al., 2016; Cunningham et al., 2005). While the segmental mirroring technique may still be used in these circumstances, it must be acknowledged that the risk of inaccuracy is increased.

Primary limitations of our study include a small sample size and lack of comparison to a patient population that had previously undergone mandibular reconstruction using this technique. In addition, we were unable to model class IV and V defects where a substantial portion of the mandible on either side of the midline required reconstruction as the extent of defect limited the ability to create a mirrored segment. Therefore, classes IV and V were excluded from our analysis. While the focus of our study was on determining the accuracy of using 3D modeling of mandibular defect classes to fashion reconstructive plates in circumstances of deforming bony pathology, we do not address the various factors involved with bone graft selection or design with respect to optimal site of harvest, placement of osteotomies, orientation etc. This was beyond the scope of our study but may be addressed in future studies. Two patients with dental artifact were excluded from our study due to difficulties with generating accurate three-dimensional reconstructions. Newer techniques for eliminating dental artifact include the use of dual-energy CT and metal artifact reduction software (Cha et al., 2017). However, this was not performed in the current study and can be considered a limitation. Lastly, an important direction for this study includes translating the described methods into a patient population using a prospective study design and comparing reconstructions using radiographic data.

5. Conclusion

While an overall high degree of conformance can be achieved when modeling the mandible using a segmental mirroring technique, variations exist that are dependent on the classification of defect. These variations should be taken into consideration when pre-planning for surgery. Inclusion of the condyle within a model will result in reduced conformance when using the mirroring technique. While modeling of class III reconstructions using the mirroring technique demonstrated the highest degree of conformity, it is important to note that this relates to the model and does not take into consideration the selected bone graft. Various case reports have reported success in using the segmental mirroring technique; however, our study represents the first to generate quantitative data regarding its accuracy. In circumstances where pathology affects the contour of the mandible, our data demonstrates that a 3D model can be generated based on symmetry from the contralateral mandibular segment with a high degree of accuracy.

Acknowledgments

This work is funded by the Guided Therapeutics (GTx) Program, University Health Network, Strobele Family GTx Research Fund, Kevin and Sandra Sullivan Chair in Surgical Oncology, Hatch Engineering Fellowship Fund, and Princess Margaret Hospital Foundation.

References

Abou-elfetouh A, Barakat A, Abdel-ghany K: Computer-guided rapid-prototyped templates for segmental mandibular osteotomies: a preliminary report. Int J Med Robot Comput Assist Surg 7: 187–192, 2011

Brown JS, Barry C, Ho M, Shaw R: A new classification for mandibular defects after oncological resection. Lancet Oncol 17(1): e23–e30, 2016

Cha J, Kim HJ, Kim ST, Kim YK, Kim HY, Park GM: Dual-energy CT with virtual monochromatic images and metal artifact reduction software for reducing metallic dental artifacts. Acta Radiol 58(1): 1312–1319, 2017

Chan H, Gilbert RW, Pagedar NA, Daly MJ, Jonathan C, Siewerdsen JH: A new method of morphological comparison for bony reconstructive surgery: maxillary reconstruction using scapular tip bone. SPIE Proc 7625: 1–2, 2010

Cohen A, Laviv A, Berman P, Nashef R, Abu-Tair J: Mandibular reconstruction using stereolithographic 3-dimensional printing modeling technology. Oral Surg Oral Med Oral Pathol Oral Radiol Endod 108(5): 661–666, 2009

Cunningham L, Madsen M, Peterson G: Stereolithographic modeling technology applied to tumor resection. J Oral Maxillofac Surg 63: 873–878, 2005

Hannen EJM: Recreating the original contour in tumor deformed mandibles for plate adapting. Int J Oral Maxillofac Surg 35: 183–185, 2006

Khalifa GA, Abd El Moniem NA, Elsayed SA-E, Qadry Y: Segmental mirroring: does it eliminate the need for intraoperative readjustment of the virtually pre-bent reconstruction plates and is it economically valuable? J Oral Maxillofac Surg 74(3): 621–630, 2016

Lee J-W, Fang J-J, Chang L-R, Yu C-K: Mandibular defect reconstruction with the help of mirror imaging coupled with laser stereolithographic modeling technique. J Formos Med Assoc 106(3): 244–250, 2007

Li J, Hsu Y, Luo E, Khadka A, Hu J: Computer-aided design and manufacturing and rapid prototyped nanoscale hydroxyapatite/polyamide (n-HA/PA) construction for condylar defect caused by mandibular angle ostectomy. Aesthet Plast Surg 35(4): 636–640, 2011

Pagedar NA, Gilbert RW, Chan H, Daly MJ, Irish JC, Siewerdsen JH: Maxillary reconstruction using the scapular tip free flap: a radiologic comparison of 3D morphology. Head Neck: 1377–1382, 2012

Singare S, Dichen L, Bingheng L, Yanpu L, Zhenyu G, Yaxiong L: Design and fabrication of custom mandible titanium tray based on rapid prototyping. Med Eng Phys 26: 671–676, 2004